ELSEVIER

Polymer 40 (1999) 2501–2510

polymer

Flow light scattering studies of polymer coil conformation in solutions under shear: effect of solvent quality

Ellen C. Lee[a,b], Susan J. Muller[a,b,*]

[a]*Department of Chemical Engineering, University of California, Berkeley, CA 94720, USA*
[b]*Center for Advanced Materials, Lawrence Berkeley National Laboratory, Berkeley, CA 94720, USA*

Received 7 April 1998; revised 28 May 1998; accepted 10 June 1998

Abstract

The orientation and deformation of polymer chains, in dilute solutions undergoing circular Couette flow, were measured by flow light scattering (FLS) techniques. Analysis of the angular dissymmetry of the scattered light intensity allowed the determination of polymer chain alignment in the flow direction, as well as a direct measurement of chain dimensions. The polymers were dissolved in several different solvents to determine the effect of solvent quality on polymer coil conformation under shear. The polymer solutions all consisted of a nearly monodisperse polystyrene sample of 3×10^6 g/mol molecular weight dissolved in various viscous solvents, including tricresyl phosphate, dioctyl phthalate, and a mixed solvent of low molecular weight polystyrene ($M_w = 5780$ g/mol) and dioctyl phthalate. There was a pronounced dependence of chain conformation on the quality of the solvent, with poorer solvents allowing more orientation of the polymers with the flow direction, as well as larger relative deformations.

Keywords: Dilute polymer solution; Light scattering; Solvent quality

1. Introduction

The understanding of chain dynamics in polymeric fluids undergoing flow has long been an aim of non-Newtonian fluid mechanics and polymer science research. It is important to understand the dynamics of isolated polymer chains, since they dictate the bulk fluid behaviour in many processing applications and are related to the mechanisms by which flow instabilities occur. Several theories are available for the predictions of such dynamics, but few experimental measures are available for comparison. While the majority of investigations have focussed on the rheological measurements of bulk fluid behaviour and simulations of isolated polymer chain dynamics, there have been few studies that detail the direct, experimental measurement of chain dynamics in real polymeric solutions. Once an understanding of isolated chain dynamics is obtained, this knowledge can also be applied to theories for concentrated solutions and melts.

The dynamics of polymer molecules in solution as a function of the solvent quality also play an important role in determining the behaviour of solutions in the complex flows of processing applications. In addition, many processing operations also include the use of mixed solvents, which are then volatilized from the product in the final processing stages. Differences in solvent qualities of the solvent components, as well as their volatilities, can affect the properties of the finished product.

Wide angle laser light scattering offers a direct method for the measurement of polymer chain dynamics. In quiescent solutions, the technique has long been used for the characterization of polymer molecular weight, second virial coefficient, and radius of gyration. The size and shape of an isolated polymer molecule can be determined by studying the angular dissymmetry of scattered light, described by the molecule's form factor or particle scattering factor. The technique can also be used for the characterization of polymer chain dynamics in flowing solutions, as first suggested by Peterlin [1,2]. A few experimental results of this type are available, including orientation of rigid rod-like particles in shear flow [3,4], dynamics of polymer chains in solution under shear flow [5–10], and polymer solutions in extensional flows [11,12]. In steady shearing flow of polymer solutions in near-Θ solvents, polymer chains were found to orient with the direction of flow according to the kinetic theory model of Zimm [5–7,10]. In addition, the Zimm model was found to correctly describe the molecular weight scaling and polydispersity dependence of the orientation

* Corresponding author.

0032-3861/99/$ - see front matter
PII: S0032-3861(98)00471-6

[10]. The amount of deformation measured by all researchers, however, was much less than predicted by any of the linear bead-spring models examined. Even in the stronger extensional flow field studied by Menasveta and Hoagland [11,12], the polymer chains showed little stretching from their equilibrium dimensions. Furthermore, Lee et al. [10] found the molecular weight scaling and polydispersity dependence of polymer chain deformation in shear flow in near-Θ solvents to be at odds with those predicted by linear bead-spring kinetic theory models.

Here, we extend the flow light scattering studies of previous work [10] to include the effects of solvent quality on the conformation of polymer chains, in steady shearing flow between concentric cylinders. The fluids studied are dilute solutions of a nominally monodisperse high molecular weight polystyrene (HMPS) in a range of viscous solvents, including dioctyl phthalate (DOP), tricresyl phosphate (TCP), and a mixture of low molecular weight polystyrene (LMPS) and dioctyl phthalate, denoted as LMPS/DOP. Both orientation and deformation of the polymer chains in this range of solvents will be discussed. It is worth noting that there are a number of system constraints that make it difficult to find suitable polymer–solvent systems for this study. These constraints include: (1) the need for a reasonably high scattering contrast between the polymer and the solvent; (2) a close refractive index match between the solvent and the glass shearing cell; (3) high solvent viscosity to allow experiments at high dimensionless shear rates at accessible rotation rates of the Couette cell; (4) a known or measurable solvent quality that spans a range from poor to Θ to good; and (5) the absence of shear-induced scattering enhancement at low values of dimensionless shear rates. These considerations motivated our selection of the mixed solvent system, LMPS/DOP.

2. Theory

2.1. Flow light scattering

Under shearing conditions that are strong enough to overcome rotational diffusion, an isolated polymer chain in solution will undergo a change from its equilibrium conformation in quiescent solution. The polymer molecule will orient to some degree with the direction of flow, and deform in size and shape. The conformation changes can be characterized by measurements of the orientation angle or orientation resistance, and chain extension and expansion ratios. The elastic dumbbell, Rouse, and Zimm kinetic theory models give predictions of the orientation angle in the following form:

$$\chi = 45^\circ + \frac{\tan^{-1}(\beta/m)}{2}, \tag{1}$$

where the orientation angle χ is defined as the angle between the major axis of the deformed polymer molecule and the direction of increasing velocity gradient (see Fig. 1). m is the orientation resistance of the polymer chains. Bossart and Öttinger [13] have shown that for light scattering, m has values of 1.0, 1.75 and 2.554 for the elastic dumbbell, Rouse and Zimm models, respectively. β in Eq. (1) is the dimensionless shear rate given by:

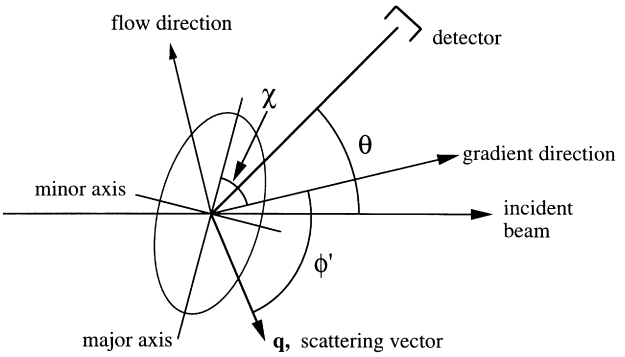

Fig. 1. Illustration of the shape of a polymer coil in shear flow. The orientation angle χ and the flow plane angle ϕ' are shown, for the specific (arbitrary) scattering angle θ and shear cell position.

$$\beta = \lambda\dot{\gamma} = \frac{[\eta]_0 \eta_s M}{RT}\dot{\gamma}, \tag{2}$$

where $[\eta]_0$ is the zero shear rate intrinsic viscosity, η_s is the solvent viscosity, M is the molecular weight, $\dot{\gamma}$ is the dimensional shear rate, R is the universal gas constant, and T is the temperature. None of these models takes into account excluded volume interactions (i.e. solvent quality effects) and, as such, are appropriate to describing the Θ condition.

The deformation of the polymer molecules is characterized by three independent coil dimensions: the major axis extension ratio, e_a; the minor axis extension ratio, e_b; and the neutral axis extension ratio, e_c. These are defined as follows:

$$e_i = \sqrt{\frac{\langle r_i^2\rangle_\beta}{\langle r_i^2\rangle_0}}, \quad i = a, b, c. \tag{3}$$

$\langle r_i^2\rangle^{1/2}$ is the major, minor or neutral axis dimension, subscript β denotes dimensions measured during shearing flow, and subscript 0 denotes quiescent conditions. The overall expansion ratio of the polymer can then be calculated from the dimensions by the following equation:

$$e = \sqrt{\frac{e_a^2 + e_b^2 + e_c^2}{3}} = \sqrt{\frac{\langle r_g^2\rangle_\beta}{\langle r_g^2\rangle_0}}, \tag{4}$$

where $\langle r_g^2\rangle^{1/2}$ is the radius of gyration of the polymer molecule. The linear bead-spring models give predictions of polymer chain deformation of the form:

$$e^2 = 1 + \frac{2}{3m}\beta^2, \tag{5}$$

with the same values of the orientation resistance as given for the orientation angle predictions. Again, these predictions do not include excluded volume effects.

2.2. Mixed solvents

For the case of the mixed solvent system, the light scattering data is more difficult to analyse than for single solvent systems. Typically, the solvent quality of each of the single solvents alone is different for the polymer in question. This may result in preferential absorption of the better solvent into the polymer chain domain, and exclusion of the second solvent. In this situation, since the local solvent mixture in the sheath surrounding the polymer chain segments is of a different composition from the solvent in the surrounding area, the excess polarizability of the polymer coil (including the absorbed solvent sheath) is not generally equal to the difference in polarizabilities between the polymer and the solvent [14]. They are only equal in the case where the solvents are isorefractive. In this case, the light scattering data can be analysed in the same way as for single solvent systems. In the system we studied, the two solvents (DOP and LMPS) are not isorefractive. Furthermore, in our system, the low molecular weight polymer species appears in appreciable concentrations, so there is concern about intermolecular interference between LMPS molecules and other LMPS or HMPS molecules, as well as the typical intramolecular interference of the HMPS molecules that is present in the single solvent systems. In Appendix A we show that, for our mixed solvent system, the light scattering can be described by the following equation:

$$\lim_{c_2 \to 0} \frac{K' c_2}{\Delta R_\theta} = \frac{1}{M_{2,\mathrm{ap}}}\left[1 + \frac{16\pi^2 n^2}{3\lambda_0^2}\langle r_g^2\rangle_{\mathrm{ap}} \sin^2(\theta/2)\right], \tag{6}$$

where c_i is the concentration of species i, ΔR_θ is the excess Rayleigh ratio, n is the refractive index of the solution, λ_0 is the wavelength of the incident laser light, and θ is the scattering angle. K' is the optical constant defined by the following equation:

$$K' = \frac{2\pi^2 n^2}{N_A \lambda_0^4}\left(\frac{\mathrm{d}n}{\mathrm{d}c_2}\right)^2, \tag{7}$$

$\langle r_g^2\rangle_{\mathrm{ap}}$ is the apparent radius of gyration of the HMPS species, defined as:

$$\langle r_g^2\rangle_{\mathrm{ap}} = \frac{\langle r_g^2\rangle}{1 - \dfrac{2M_1^2 A_{2,11}^{(1)}(c_1)c_1^2}{M_2[1 - 4M_1 A_{2,12}(c_1, c_2)c_1]}}, \tag{8}$$

and $M_{2,\mathrm{ap}}$ is the apparent molecular weight of the HMPS, defined as:

$$M_{2,\mathrm{ap}} = M_2[1 - 4M_1 A_{2,12} c_1 - 2M_1^2 M_2^{-1} A_{2,11}^{(1)}(c_1)c_1^2]. \tag{9}$$

In the above, the subscript 1 refers to the LMPS and 2 refers to the HMPS. The second virial coefficients that appear in Eqs. (8) and (9) are defined in the appendix. Since the multicomponent light scattering equations have the same form as the binary system equations, the flow light scattering in the mixed solvent system can, therefore, be analysed in the same way as the single solvent light scattering data.

3. Experimental

3.1. Materials

The solutions for the flow light scattering study were composed of nearly monodisperse, high molecular weight polystyrene (HMPS) of 3×10^6 g/mol, dissolved in one of three viscous solvents: dioctyl phthalate, tricresyl phosphate (both from Aldrich), or a mixed solvent of DOP and low molecular weight polystyrene (LMPS, $M_w = 5780$ g/mol), denoted as LMPS/DOP. Intrinsic viscosity measurements for the HMPS/TCP system were performed on solutions of nearly monodisperse polystyrenes of the following molecular weights (in g/mol): 6.7×10^5, 9.0×10^5, 1.5×10^6, 2.0×10^6 and 2.0×10^7; for the HMPS/DOP system at $T = 13$°C, nearly monodisperse polystyrenes of the following molecular weights were used (in g/mol): 1.29×10^5, 4.0×10^5, 7.0×10^5, 1.5×10^6 and 3×10^6. All polymer samples had polydispersity indices of $M_w/M_n \leq 1.30$ and were obtained from Pressure Chemical. Spectrophotometric grade toluene was purchased from Fisher Chemical, and decahydronaphthalene (decalin) for the refractive index matching bath for the light scattering experiments was obtained from Aldrich.

3.2. Sample preparation

For intrinsic viscosity measurements, the samples were used with no further preparation of either polymer or solvent. Samples for light scattering were prepared by the following procedure. The polymer was first dissolved in spectrophotometric grade toluene filtered through 0.2 μm pore size PTFE syringe filters (Gelman Sciences). The resulting solutions were then filtered a second time through 1.0 μm filters (Whatman). The toluene was volatilized from the solutions in a vacuum oven at 40°C to obtain a clean, dry polymer. The viscous solvent was then filtered through 0.2 μm pore size filters and added to the dry polymer. For the mixed solvent system, the mixed solvent was prepared in the manner as described above, and then added to the clean, dry polymer without further filtration. The mixed solvent consisted of 13 wt% LMPS and 87 wt% DOP. This is the same solvent used by Solomon and Muller, who reported intrinsic viscometry and quiescent static and dynamic light scattering results [15].

3.3. Intrinsic viscometry

The solvent qualities of the various solutions were evaluated by intrinsic viscosity measurements and characterized by an excluded volume exponent, ν, defined by the scaling relationship $\langle r_g^2\rangle^{1/2} \sim M^\nu$. Thus, $\nu = 0.5$ indicates Θ conditions, $\nu > 0.5$ for good solvents and $\nu < 0.5$ for poor solvents. The intrinsic viscosity measurements were determined from fall times measured in a Schott Automatic Viscometer (AVS 350), using an Ubbelohde viscometer

and LED photo-diode detectors. The viscometer was immersed in a recirculating water bath that regulated the temperature to within 0.1°C. For the more viscous mixed solvent, independent viscosity measurements on a torsional viscometer (Rheometrics RFS with a Couette cell fixture) verified that the intrinsic viscosity was independent of the shear rate, over the range of shear rates produced in the capillary [15]. In the less viscous single solvents, for all but the highest molecular weight sample in TCP, an estimate of the dimensionless shear rate β in the capillary of the viscometer suggest that the measured intrinsic viscosities correspond to zero-shear-rate values. For the 2×10^7 g/mol polystyrene in TCP, an estimate of β in the capillary is approximately 20, suggesting that the zero-shear-rate intrinsic viscosity may be somewhat higher than the measured value. This point was omitted in the determination of the excluded volume exponent ν.

3.4. Light scattering

Static light scattering experiments were performed on a Brookhaven Instruments system equipped with an Innova 70-2 argon ion laser, with wavelength $\lambda_0 = 488$ nm. Quiescent solution samples were held in Pyrex sample cells of 13 mm nominal diameter. Sample cells were immersed in decalin for refractive index matching. The temperature was regulated by a recirculating water bath to within 0.1°C. The refractive index increment for the HMPS/TCP system required for light scattering measurements was determined to be $dn/dc = 0.0417$ ml/g using a Brice–Phoenix differential refractometer equipped with a mercury arc lamp (and interpolating to the wavelength of the light scattering experiments). For the HMPS/DOP system $dn/dc = 0.1095$ ml/g, and for the HMPS/LMPS/DOP system $dn/dc_2 = 0.0980$ ml/g. Zimm plots were constructed from the quiescent solution light scattering measurements for each of the polymer–solvent systems. The concentration range used for the quiescent solution light scattering experiments was between $0.015c^* \leq c \leq 0.384c^*$. Scattering angles were varied between $40° \leq \theta \leq 140°$, giving scattering vectors between $1.31 \times 10^{-2}\ \text{nm}^{-1} \leq |\mathbf{q}| \leq 3.60 \times 10^{-2}\ \text{nm}^{-1}$ for DOP and LMPS/DOP solutions, and $1.37 \times 10^{-2}\ \text{nm}^{-1} \leq |\mathbf{q}| \leq 3.76 \times 10^{-2}\ \text{nm}^{-1}$ for TCP solutions.

3.5. Flow light scattering

A detailed description of the apparatus and techniques for the flow light scattering experiments are available in a previous publication [10]. In addition to the shear cell used for the FLS experiments in the previous publication, an additional concentric cylinder Couette cell was fashioned for the light scattering studies in TCP, for refractive index matching considerations. Both inner and outer cylinders were constructed of G12 glass with a refractive index of $n_{D,glass} = 1.55$, purchased from Wilmad Glass. The refractive index of TCP is $n_{D,TCP} = 1.555$. The inner cylinder was constructed from a piece of glass tubing, closed on top by a stainless steel shaft and on the bottom by an anodized aluminium cap. The cylinder was then filled with TCP to improve the refractive index match at the glass–liquid interface. The outer diameter of the inner cylinder was 28.575 mm. The outer cylinder had an inner diameter of 31.75 mm and was closed on the bottom by an anodized aluminium cap. The shear cell was also immersed in TCP in the light scattering vat to serve both index matching and temperature control purposes. The geometry of the set-up and a schematic of the apparatus are shown in Fig. 2a and b.

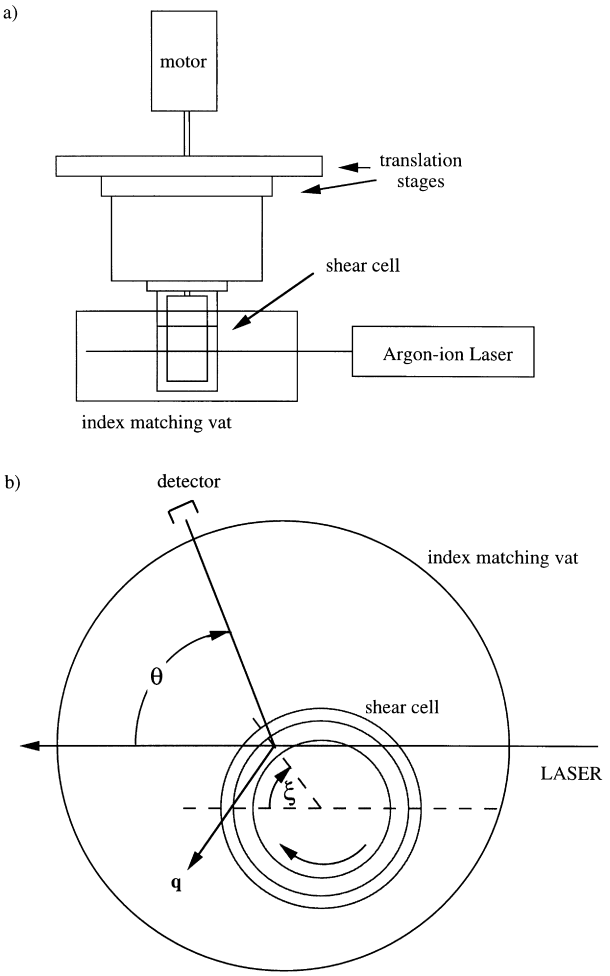

Fig. 2. Flow light scattering apparatus: (a) side view, and (b) top view; ξ is the shear cell position.

For both HMPS/DOP ($n_{D,DOP} = 1.486$) and HMPS/LMPS/DOP ($n_{D,LMPS/DOP} = 1.498$) systems, the original Couette shear cell constructed of Corning 7740 glass was used ($n_{D,glass} = 1.474$). The outer cylinder had an inner diameter of 33 mm, while the inner cylinder was a solid glass rod with a diameter of 30 mm. The shear cell for these experiments was immersed in decalin in the light scattering vat, for index matching and temperature control.

The orientation angle experiments were performed in a similar fashion as described in Ref. [10]. The intensity of the light scattered by the sheared solutions was taken as a

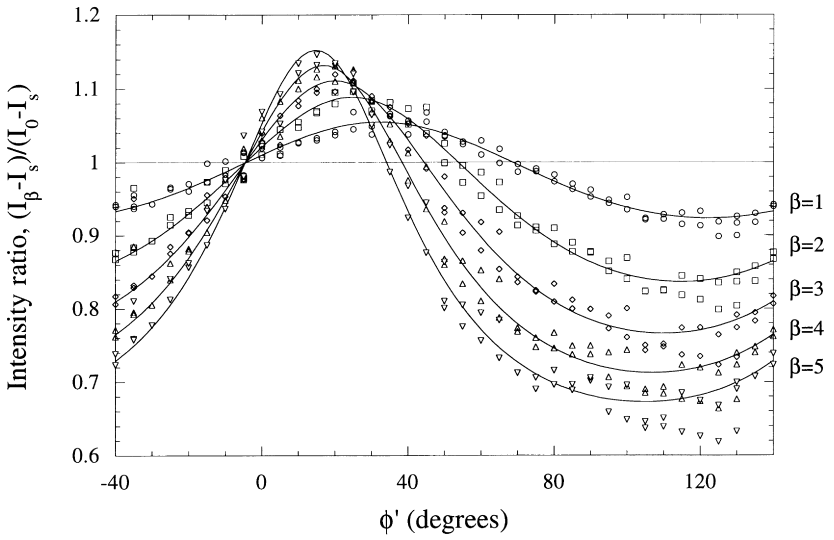

Fig. 3. Intensity ratio versus flow plane angle for various shear rates for 3×10^6 g/mol HMPS/DOP at $T = 25$°C and $\theta = 80°$.

function of the flow plane angle, ϕ' (see Fig. 1), the angle described by the gradient direction and the scattering vector. The sheared solution light intensity measurements were then normalized by those of the quiescent solution. The orientation angle, χ, of the polymer coils in dilute solution was then determined from the intensity data by the maximum of the intensity ratio curve (see Fig. 3). As shown by Link and Springer [6,7], orientation angle measurements were sensitive to concentration effects above $0.2c^*$, where c^* is the overlap concentration determined by $1/[\eta]_0$. In 1997, Lee et al. [10] also found that in all solutions of HMPS/DOP studied — all below $0.165c^*$ — concentration effects were negligible. In the present studies, the concentrations of the solutions examined were dictated by the size of the refractive index increment of the given system. For solutions with smaller dn/dc, higher concentrations were necessary to provide the contrast in polymer versus solvent scattering. All solutions examined here were kept below $0.2c^*$ (see Table 1 for details), such that concentration effects remained negligible.

The deformation experiments were analysed using a Zimm-plot-type analysis. In a quiescent solution Zimm plot experiment, intensity data are collected at several detection angles, θ, for several concentrations of polymer in solution. Weight average molecular weight, radius of gyration, and second virial coefficient information are then obtained by performing a double extrapolation to $c = 0$ and $\theta = 0°$. For the shear experiments, the Zimm-plot-type analysis requires data to be taken in the same manner, while keeping $\phi' = \chi$ for major axis deformation, or $\phi' = \chi + 90°$ for minor axis deformation. Fig. 4 shows a quiescent solution Zimm plot for the 3×10^6 g/mol HMPS/DOP solution at $T = 25$°C, with shear data for the major axis at $\beta = 3.17$ overlaid. The major axis extension ratio is determined from

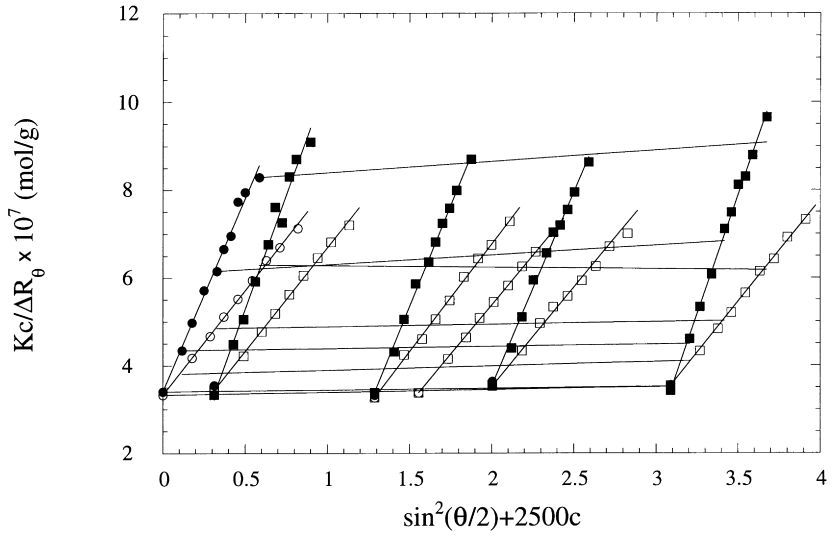

Fig. 4. Quiescent solution Zimm plot (open markers) with shear data for the major axis at $\beta = 3.17$ (filled markers), overlaid for 3×10^6 g/mol HMPS/DOP at $T = 25$°C.

Table 1
Refractive index increments for various systems and concentrations used for orientation angle experiments

System	Temperature (°C)	Concentration (c/c^*)	dn/dc (ml/g)
HMPS/TCP	25	0.199	0.0417
HMPS/DOP	25	0.069	0.1095
HMPS/DOP	13	0.062	0.1095
HMPS/LMPS/DOP	25	0.173	0.0980

the ratio of the slope of the infinite dilution lines in shear to zero shear, with a similar procedure for the minor axis extension ratio. Although a strict analysis requires extrapolation to infinite dilution, as seen here, previous experiments in HMPS/DOP solutions showed that extrapolations to $c = 0$ were unnecessary when concentrations were kept below $0.1c^*$ [10].

4. Results

4.1. Solvent quality

The solvent qualities of all the HMPS solutions were first characterized by intrinsic viscometry experiments. Shown in Fig. 5 are the molecular weight scalings of intrinsic viscosity for the HMPS/TCP and HMPS/DOP (at $T = 13$°C) systems. Also reproduced here are the data from Solomon and Muller [15] for the scaling of the HMPS/LMPS/DOP system. From the Mark–Houwink exponents, we see that TCP is a good solvent for HMPS, and that DOP (at $T = 13$°C) and the mixed solvent LMPS/DOP are poor solvents. In addition to intrinsic viscometry, Solomon and Muller show that the mixed solvent is poor in quality through dynamic light scattering and rheometry experiments [15]. The solvent qualities of poor and near-Θ systems were further characterized by observations of the onset of shear-induced scattering enhancement seen by the present authors. Critical shear rates, β_{crit}, were assigned for solutions of 3×10^6 g/mol HMPS in the flow light scattering apparatus, by the appearance of a sudden increase in the scattering intensity as the shear rate was increased beyond the critical. The earlier onset of scattering enhancement, whether due to shear-induced concentration fluctuations [16–20] or a coil-globule transition, is related to the decreasing solvent quality of the system. It is noted here that the good solvent system HMPS/TCP showed no shear-induced scattering enhancement. Both excluded volume exponents and critical shear rates for the various systems are listed in Table 2. Also included in Table 2 is the excluded volume exponent for the HMPS/DOP (at $T = 25$°C) system taken from Link and Springer [7].

4.2. Orientation

The orientation angle as a function of solvent quality was determined by the location of the maximum in an intensity ratio curve, as seen in Fig. 3 and described more fully in Lee et al. [10]. By the geometry of the set-up, the orientation angle χ is given by $\chi = 90° - \phi'_{max}$, where ϕ'_{max} is the value of ϕ' at which the intensity ratio is at a maximum. As shown in Fig. 6a, the orientation of the polymer molecules with the flow direction becomes more complete as the solvent quality is decreased. The polymer shows slightly less orientation in the good solvent TCP than in the near-Θ solvent DOP. Similarly, as we further decrease the solvent quality to DOP at $T = 13$°C and then to the mixed solvent case, we obtain larger orientation angles. The orientation angle is shown as a function of dimensionless shear rate β, and is also compared with kinetic theory predictions. While these

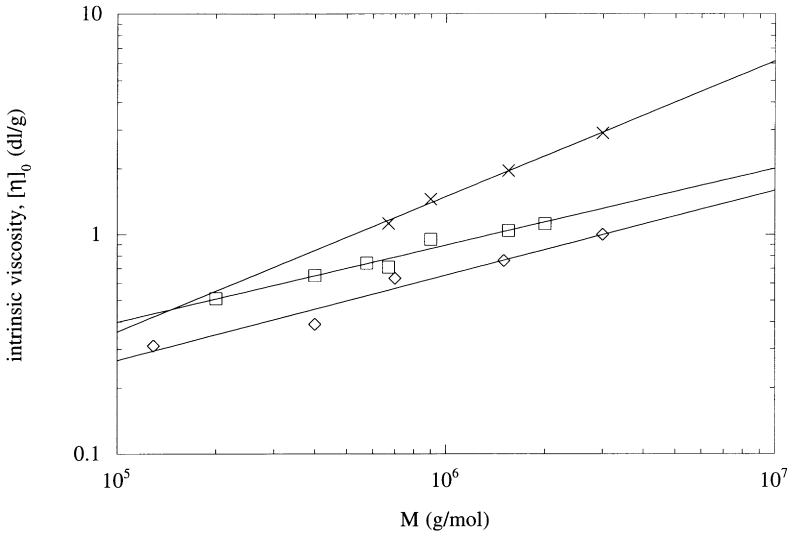

Fig. 5. Molecular weight scalings of intrinsic viscosity for HMPS/TCP (X), HMPS/LMPS/DOP[15] (□) and HMPS/DOP at $T = 13$°C (◇). The parameters for the Mark–Houwink equation, $[\eta]_0 = KM^a$, are obtained from the linear fits. The regressions give the following parameters: $[\eta]_0 = 3.0 \times 10^{-4}$ dl/g $M^{0.62}$ for HMPS/TCP, $[\eta]_0 = 7.0 \times 10^{-3}$ dl/g $M^{0.35}$ for HMPS/LMPS/DOP, and $[\eta]_0 = 3.0 \times 10^{-3}$ dl/g $M^{0.39}$ for HMPS/DOP (at $T = 13$°C).

Table 2
Measures of solvent quality for HMPS in various solvents. Excluded volume exponents ν determined by intrinsic viscometry. Critical shear rates β_{crit} for the onset of shear-induced scattering enhancement for 3×10^6 g/mol HMPS solutions determined by light scattering in a Couette shear cell

Solvent	Temperature (°C)	η_s (mPa/s)	Excluded volume exponent, ν	β_{crit}
TCP	25	62.5	0.54	Not applicable
DOP	25	61	0.51[a]	8.7
DOP	13	137	0.46	6.9
LMPS/DOP	25	139	0.45[b]	4.7

[a]From Ref. [7].
[b]From Ref. [15].

models do not give predictions for solvent quality effects, they do show the qualitative behaviour of the shear rate dependence of the polymer chain orientation. Further, the Zimm model predictions agree almost quantitatively with measurements at near-Θ conditions. The orientation resistance parameter, *m*, of these samples is also shown as a function of the shear rate (Fig. 6b). The orientation resistance increases as the shear rate is increased, as seen by other researchers [6,8,9,21]. That is, the polymer chains become increasingly difficult to orient as the shear rate is

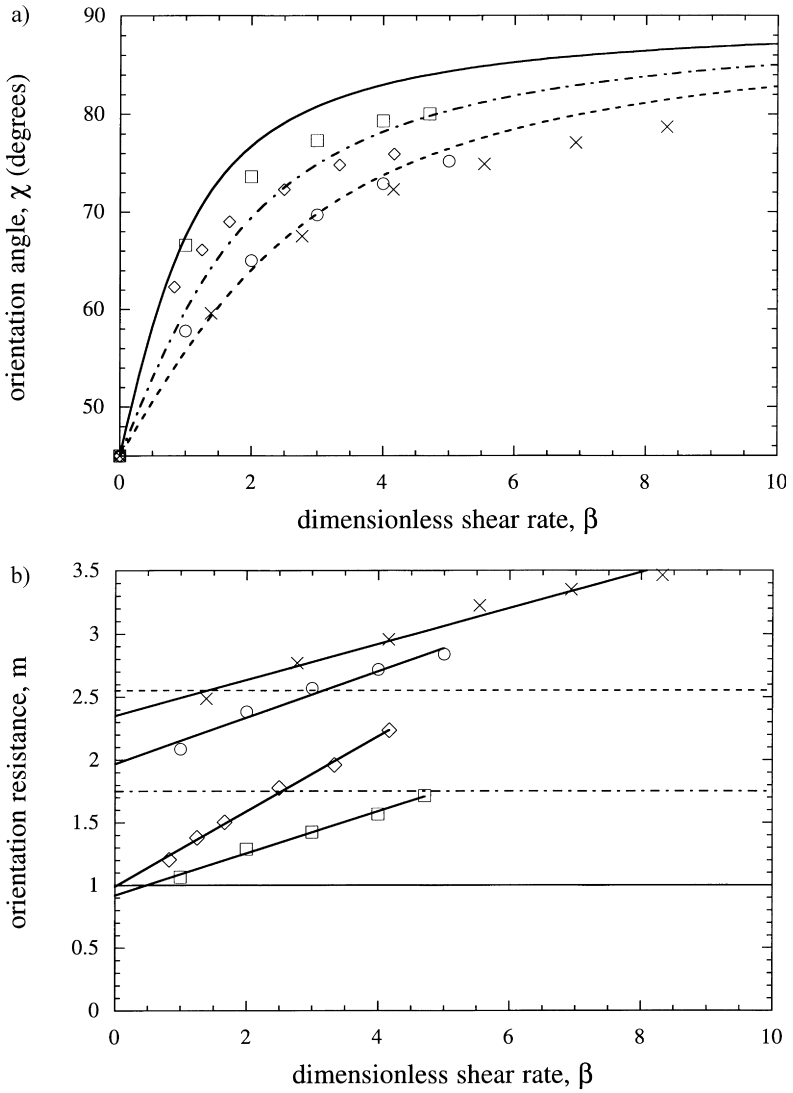

Fig. 6. Polymer chain orientation angle χ (a) and polymer chain orientation resistance *m* (b), versus shear rate β for HMPS/TCP (X), HMPS/DOP at $T = 25$°C (○), HMPS/DOP at $T = 13$°C (◇) and HMPS/LMPS/DOP (□). Kinetic theory models included for comparison. Elastic dumbbell model (-), Rouse model (– · –) and Zimm model (- - -).

increased. Additionally, the values for m are systematically lower for the solvents of poorer quality.

4.3. Deformation

The effect of solvent quality on deformation of the chains was assessed by comparing the overall expansion ratio, e, of the polymers in each solution. The overall expansion ratios were determined from the major and minor axis extension ratios by a Zimm-plot-type analysis, as described previously [10], with the neutral axis extension ratio e_c assumed to be unity. This assumption of constancy of chain dimensions in the neutral direction has been confirmed experimentally by Link and Springer [6,7]. A sample plot showing the major axis extension ratio (as a ratio of the slopes of the shear to quiescent solution data extrapolated to zero concentration) is shown in Fig. 4. Fig. 7 shows the polymer chain deformation as a function of solvent quality and shear rate. The polymer chains in the poor, mixed solvent case undergo the most deformation, and those in the good solvent TCP case undergo the least deformation. Also shown in the plot are predictions from kinetic theory models. As seen in the previous work, as well as by other researchers [5–9,22], the measured deformation is much less than predicted by the linear bead-spring models for all polymer–solvent systems. In both orientation and deformation experiments, the upper limit of the dimensionless shear rate for the near-Θ and poor solvents is determined by the onset of shear-induced scattering enhancement. Larger dimensionless shear rates, however, were achievable for the good solvent system of HMPS/TCP, as a result of the absence of shear-induced scattering enhancement.

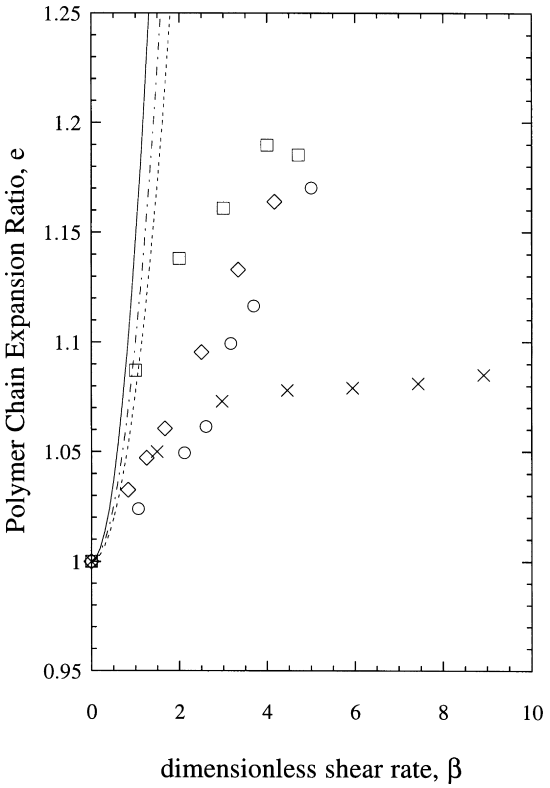

Fig. 7. Polymer chain expansion ratio e versus shear rate β for various solvent systems. Symbols are for the same samples as in Fig. 6.

5. Discussion

In the present study, we have examined the effect of solvent quality on the conformation of polymer chains in dilute solution. For the four solvents studied, the orientation of the polymer molecules with the flow direction increases monotonically with decreasing solvent quality. The good solvent TCP allowed the polystyrene molecules to align less at a given shear rate than the near-Θ solvent DOP at $T = 25$°C. When we consider DOP at a lower temperature, where it acts as a poor solvent, the shift towards more complete orientation with the flow direction (less orientation resistance m) is unambiguous (see Fig. 6b). Consistent with the trend, the mixed solvent, which is a slightly poorer solvent than DOP at $T = 13$°C, shows even less orientation resistance. The ordering of the orientability of the polymers in solution is consistent with our ranking of the solvent qualities, as examined both by observations of shear-induced scattering enhancement (β_{crit}) and intrinsic viscometry (excluded volume exponents).

Previous work has been carried out by Zisenis and Springer [6,8,9,21] concerning the effect of solvent quality on polymer chain orientation in shear flow, who found that as they improved the quality of the solvent, the orientation resistance m decreased, and the polymer chains aligned more completely with the direction of flow. The trend, however, was not strictly monotonic with the solvent power. While this is in contrast to the results we present here, the origin of the discrepancy remains unclear. It is worth noting that our results for DOP at $T = 25$°C, overlay well with the results Zisenis and Springer obtained for the same system. The solutions studied by Zisenis and Springer are mixed solvent systems of good solvent quality and near-Θ or good single solvents. In addition to the fact that we are looking mostly at near-Θ and poorer-than-Θ solvents, while Zisenis and Springer are examining near-Θ and good solvents, our solvents are, in general, much more viscous than theirs (by a factor of over 30 in some cases). Hence, a detailed comparison of the two data sets might provide insights into the differing effects of thermodynamics and hydrodynamic interactions on the orientation of polymer chains in shear flow.

When the orientation resistance trends in our work are compared with birefringence experiments carried out by Bossart and Öttinger [23], the trend with solvent quality agrees with their findings. In these experiments, however, they stayed at extremely low shear rates (their apparatus allowed orientation angle determination at very low shear rates with good accuracy), such that the differences between

the orientation resistance for their good solvent and Θ solvent were very slight.

In terms of polymer chain deformation, the polymers dissolved in the poor solvents show more deformation from the equilibrium conformation than polymers in better solvents. While Zisenis and Springer do not show data for deformation measurements for a range of solvent qualities, our results for polystyrene in the near-Θ solvent DOP (at $T = 25°C$) are consistent with their deformation measurements in that system; a detailed comparison is presented in Fig. 8 of Ref. [10]. The present results are in contrast to the calculations of Bruns and Carl [24], who solve the Langevin equations for the Rouse and Zimm models with and without excluded volume, subject to a linearization approximation that allows pre-averaging of hydrodynamic interactions. Their calculations predict larger deformations in good solvents than in Θ solvents. We note, however, that substantially more deformation is predicted even in Θ solvents than is consistent with either our results or those of Springer and coworkers.

One possibility is that the effect of solvent quality on the deformation of the polymer chains is due to the shear rate dependence of the intrinsic viscosity at the high shear rates of the Couette cell experiments. As shown by Noda et al. [25], the shear-thinning behaviour of dilute polymer solutions depends on both excluded volume effects and chain flexibility. Excluded volume effects are increased for better solvents, increasing the shear-thinning nature of the intrinsic viscosity. In other words, for the better solvents, we anticipate the shear-thinning in $[\eta]$, and hence λ, to be more profound than for the poorer solvent systems. In presenting our data, we have used a scaling consistent with the linear bead-spring models, where the relaxation time (and $[\eta]$) is independent of the shear rate. Perhaps a more appropriate scaling is one based on a shear-rate-dependent relaxation time or $[\eta]$. If all the data were replotted as a function of $\lambda(\dot{\gamma})\dot{\gamma}$ rather than $\lambda_0\dot{\gamma}$, the better solvent results would be shifted to a greater degree to smaller values, and would perhaps overlay the poorer solvent results.

A second possibility is that the extended conformation of the polymer chains is less sensitive to solvent quality than the equilibrium conformation. Then the high β asymptotic value of the expansion ratio e for a poor solvent would be higher, as a result of the lower value of the equilibrium (quiescent) radius of gyration. This is consistent, at least, with our deformation data for the good solvent TCP. For TCP, the expansion ratio e appears to reach a constant value of ~1.08 at $\beta \approx 5$. For the polystyrene sample considered, for which the equilibrium radius of gyration in TCP is 63 nm, this corresponds to a radius of gyration under shear of approximately 68 nm. In the poor solvent DOP at $T = 13°C$, where the same polymer has an equilibrium radius of gyration of 50 nm, we would anticipate a high β deformation ratio of 1.36 if the extended conformation is independent of solvent quality.

In summary, the present results show that the effect of solvent quality is quite significant and should not be neglected in the prediction of polymer chain dynamics in solution. A change in the solvent quality results in changing both thermodynamic and hydrodynamic interactions. Although the physical origin of the effects of solvent quality remain unclear, the results do show that they must be accounted for in the kinetic theory models, in order to describe accurately polymer chain orientation and deformation.

Acknowledgements

This work was supported in part by the Director, Office of Energy Research, Office of Basic Energy Sciences, Materials Sciences Division of the US Department of Energy, under contract no. DE-AC03-76SF00098. The authors also wish to acknowledge gifts to support polymer research from Raychem.

Appendix A Mixed solvent systems

Light scattering data in polymer–mixed solvent systems are more complicated to analyse than for single solvent systems. Theories for light scattering in multicomponent systems have been derived independently by Kirkwood and Goldberg [26] and by Stockmayer [27], who were mainly concerned with the effect on the thermodynamics. Yamakawa [28,29] extended these theories to include the effects of multiple components on the light scattering interference functions. Owing to the difference in solvent qualities and polarizabilities of the various components in solution, the excess polarizability of the main polymer species is no longer, in general, equal to the difference in polarizabilities between that polymer species and the remaining components. Further, one must consider both inter- and intramolecular interference between all components.

Following the construction of Yamakawa [28,29], the light scattering equation in ternary systems of a high polymer in a mixed solvent of low molecular weights is then of the following form:

$$\begin{aligned}\frac{\Delta R_\theta}{K' M_2 c_2} &= P_{1,2}(\theta, c_1, c_2) - 2M_2 A_{2,22}(c_1, c_2) P_{2,22}(\theta, c_1, c_2) c_2 \\ &\quad - 4\gamma M_1 A_{2,12}(c_1, c_2) P_{2,12}(\theta, c_1, c_2) c_1 - 2\gamma^2 M_1^2 M_2^{-1} \\ &\quad \times [A_{2,11}(c_1, c_2) P_{2,11}(\theta, c_1, c_2) - A_{2,11}(c_1) \\ &\quad \times P_{2,11}(\theta, c_1)] c_1^2 c_2^{-1}, \end{aligned} \tag{A1}$$

where the subscript 1 refers to the second solvent (LMPS), and the subscript 2 the polymer (HMPS), ΔR_θ is the excess Rayleigh ratio of the polymer over that of the mixed solvent, M_i is the molecular weight of species i, $P_{1,i}$ is the intramolecular interference function for species i, $P_{2,ij}$ is the

intermolecular interference function between species i and j, $A_{2,ij}$ is the second virial coefficient between species i and j, c_i is the concentration of species i, and θ is the scattering angle. K' is an optical constant given by:

$$K' = \frac{2\pi^2 n^2}{N_A \lambda_0^4}\left(\frac{\mathrm{d}n}{\mathrm{d}c_2}\right)^2, \tag{A2}$$

where n is the refractive index of the solution and λ_0 is the wavelength of incident laser light. γ is defined by the following equation:

$$\gamma = \frac{\left(\frac{\mathrm{d}n}{\mathrm{d}c_1}\right)_{T,P,c_2}}{\left(\frac{\mathrm{d}n}{\mathrm{d}c_2}\right)_{T,P,c_1}}. \tag{A3}$$

The numerator refers to the change in refractive index of the solvent mixture as a function of concentration of species 1 (here, LMPS). The denominator is the change in refractive index of the solution as a function of concentration of species 2 (here, HMPS) [15]. When the solvents are isorefractive, $\gamma = 0$ and the system can be analysed in the usual way. In our system, since the LMPS and HMPS are chemically identical, $\gamma = 1$. In the limit of $\theta = 0$, the interference functions approach unity, such that Eq. (A1) yields the following:

$$\lim_{\theta\to 0}\frac{K'c_2}{\Delta R_\theta} = \frac{1}{M_{2,\mathrm{ap}}} + 2A_{2,\mathrm{ap}}c_2 + \ldots \tag{A4}$$

$M_{2,\mathrm{ap}}$ is the apparent molecular weight of the HMPS species and $A_{2,\mathrm{ap}}$ is the apparent second virial coefficient, defined as follows:

$$M_{2,\mathrm{ap}} = M_2(1 - 4M_1A_{2,12}c_1 - 2M_1^2M_2^{-1}A_{2,11}^{(1)}(c_1)c_1^2) \tag{A5}$$

$$A_{2,\mathrm{ap}} = A_{2,22}(c_1)(1 + 4M_1A_{2,12}c_1 + \ldots)$$

In the limit of infinite dilution for HMPS ($c_2 = 0$) and isotropic scattering for the mixed solvent, Eq. (A1) can be rearranged to give:

$$\lim_{c_2\to 0}\frac{K'c_2}{\Delta R_\theta} = \frac{1}{M_{2,\mathrm{ap}}}\left[1 + \frac{16\pi^2 n^2}{3\lambda_0^2}\langle r_\mathrm{g}^2\rangle_{\mathrm{ap}}\sin^2(\theta/2)\right], \tag{A6}$$

$\langle r_\mathrm{g}^2\rangle_{\mathrm{ap}}$ is the apparent radius of gyration of the HMPS species, defined as:

$$\langle r_\mathrm{g}^2\rangle_{\mathrm{ap}} = \frac{\langle r_\mathrm{g}^2\rangle}{1 - \dfrac{2M_1^2A_{2,11}^{(1)}(c_1)c_1^2}{M_2[1 - 4M_1A_{2,12}(c_1,c_2)c_1]}}. \tag{A7}$$

Eqs. (A4) and (A6) imply that we can now use the usual light scattering analysis to extract measurements of the apparent values for the molecular weight, second virial coefficient, and radius of gyration of the HMPS in the mixed solvent. By knowledge of the second virial coefficient for the LMPS in DOP, as well as the cross coefficient for LMPS and HMPS in the mixed solvent (constants in the flow light scattering experiments), we can determine the actual values for M_w, A_2, and $\langle r_\mathrm{g}^2\rangle^{1/2}$. However, for the flow light scattering experiments, since we are only looking at relative changes in the radius of gyration as a function of the shear rate, the absolute values of the virial coefficients are not necessary.

References

[1] Peterlin A. J Polym Sci 1957;23:189.
[2] Peterlin A, Heller W, Nakagaki M. J Chem Phys 1958;28:470.
[3] Heller W. Rev Modern Phys 1959;31:1072.
[4] Doppke HJ, Heller W. J Colloid Interface Sci 1967;25:586.
[5] Cottrell FR, Merrill EW, Smith KA. J Polym Sci, Part A-2 1969; 7:1415.
[6] Link A, Zisenis M, Protzl B, Springer J. Makromol Chem, Macromol Symp 1992;61:358.
[7] Link A, Springer J. Macromolecules 1993;26:464.
[8] Zisenis M, Springer J. Polymer 1994;35:3156.
[9] Zisenis M, Springer J. Polymer 1995;36:3459.
[10] Lee EC, Solomon MJ, Muller SJ. Macromolecules 1997;30:7313.
[11] Menasveta MJ, Hoagland DA. Macromolecules 1991;24:3427.
[12] Menasveta MJ, Hoagland DA. Macromolecules 1992;25:7060.
[13] Bossart J, Öttinger HC. Macromolecules 1995;28:5852.
[14] Flory PJ. Principles of polymer chemistry. Ithaca, NY: Cornell University Press, 1953.
[15] Solomon MJ, Muller SJ. J Polym Sci, Polym Phys Ed 1996;34:181.
[16] van Egmond JW, Fuller GG. Macromolecules 1993;26:7182.
[17] van Egmond JW, Werner DE, Fuller GG. J Chem Phys 1992;96:7742.
[18] Yanase H, Modenaers P, Mewis J, Abetz V, van Egmond JW, Fuller G. Rheol Acta 1991;30:89.
[19] Rangel-Nafaile C, Metzner AB, Wissbrun KF. Macromolecules 1984;17:1187.
[20] Ver Strate G, Philippoff W. J Polym Sci, Polym Lett Ed 1974;12:267.
[21] Zisenis M. Eur Polym J 1997;33:773.
[22] Cottrell FR. An experimental study of the conformation of polyisobutylene in a hydrodynamic shear field, PhD thesis, Massachusetts Institute of Technology, MA, 1968.
[23] Bossart J, Öttinger HC. Macromolecules 1997;30:5527.
[24] Bruns W, Carl W. Macromolecules 1993;26:557.
[25] Noda I, Yamada Y, Nagasawa M. J Chem Phys 1968;72:2890.
[26] Kirkwood JG, Goldberg RJ. J Chem Phys 1950;18:54.
[27] Stockmayer WH. J Chem Phys 1950;18:58.
[28] Yamakawa H. J Chem Phys 1967;46:973.
[29] Yamakawa H. Modern theory of polymer solutions. New York: Harper and Row, 1971.